

## Multi-criterion methods to extract topographic feature lines from contours on different topographic gradients

Lu Cheng, Qingsheng Guo, Lifan Fei, Zhiwei Wei, Guifang He & Yang Liu

To cite this article: Lu Cheng, Qingsheng Guo, Lifan Fei, Zhiwei Wei, Guifang He & Yang Liu (2022): Multi-criterion methods to extract topographic feature lines from contours on different topographic gradients, International Journal of Geographical Information Science, DOI: [10.1080/13658816.2021.2024194](https://doi.org/10.1080/13658816.2021.2024194)

To link to this article: <https://doi.org/10.1080/13658816.2021.2024194>



Published online: 13 Mar 2022.



Submit your article to this journal [↗](#)



View related articles [↗](#)



View Crossmark data [↗](#)



RESEARCH ARTICLE



# Multi-criterion methods to extract topographic feature lines from contours on different topographic gradients

Lu Cheng<sup>a</sup>, Qingsheng Guo<sup>a,b</sup> , Lifan Fei<sup>a</sup>, Zhiwei Wei<sup>c</sup> , Guifang He<sup>d</sup> and Yang Liu<sup>a</sup>

<sup>a</sup>School of Resource and Environmental Sciences, Wuhan University, Wuhan, China; <sup>b</sup>State Key Laboratory of Information Engineering in Surveying, Mapping and Remote Sensing, Wuhan University, Wuhan, China; <sup>c</sup>Key Laboratory of Network Information System Technology (NIST), Aerospace Information Research Institute, Chinese Academy of Sciences, Beijing, China; <sup>d</sup>School of Geographic Information and Tourism, Chuzhou University, Anhui, China

## ABSTRACT

The existing methods of the automatic extraction of topographic feature lines from terrain representation either have too high sensitivity to terrain noise or lose significant branches. In this study, we present new multi-criterion methods to extract topographic feature lines from contours on different topographic gradients according to the negative or positive signs of the curvature and neighboring feature points on the contours, the hierarchical structure of these feature points, and the spatial relationships between topographic feature lines and contours. First, the digitization directions of source contours were automatically detected and adjusted (when necessary) to establish the spatial relationships among the contours before we extract and group the feature points in the terrain. Second, we determine the 'mainstreams' and 'tributaries' of the topological structure trees according to the relationships among the previously identified feature point groups. Finally, a key aspect of our paper is the proposition of multi-criterion methods to extract topographic feature lines. Compared with the regular square grids (RSG)-based and Voronoi skeleton-based methods, the proposed methods can extract topographic feature lines with higher accuracy, better continuity, lower spatial logical conflicts between topographic feature lines and contours.

## ARTICLE HISTORY

Received 10 May 2019  
Revised 24 December 2021

## KEYWORDS

Contours; multi-criterion methods; topographic feature lines

## 1. Introduction

In geomorphology, the topographic feature lines (valley and ridge lines), where the water flows potentially converges or diverges, are skeleton lines that demarcate the terrain forms in the studied region (Hu *et al.* 2002). The correct extraction of topographic feature lines plays an important role in the hydrographical analysis, cartography and recognition of geomorphology of a given area and the establishment of grid digital elevation models (DEMs) (Mark 1984, Band 1986, Weibel 1992). Scholars in

various countries have been trying to study and discuss this problem by using various methods based on different data sources.

DEMs have different concrete types, such as regular square grids (RSG), triangulated irregular networks (TIN) and contours (Tang 2010). At present, the method of extraction of topographic feature lines using RSG is the most popular approach. Luo and Stepinski (2008) divided the RSG-based methods into hydrology-based and morphology-based methods. In the hydrology-based method, using the D8 flow direction algorithm is the simplest method; its main associated channelization criteria are the contributing area threshold (O'Callaghan and Mark 1984), stream order threshold (Peckham 1995), contributing area and the slope threshold (Montgomery and Dietrich 1992), contributing area and the stream length threshold. Even so, such algorithms can hardly detect the geologic contrast from the changing patterns of landscape dissection (Luo and Stepinski 2008). Therefore, Molloy and Stepinski (2007) proposed the terrain morphology-based method, which detects incision directly from the terrain morphology rather than relying on flow directions and channelization criteria. Moreover, Jasiewicz and Metz (2011) presented new GRASS GIS (geographic resources analysis support system, geographic information system) software toolkit to work with drainage systems modeled with multiple flow direction algorithms, which overcomes the limitations of the aforementioned methods. Recently, with the availability of high-resolution digital topographic data obtained by airborne laser scanning, certain scholars have employed different ways to extract feature lines, eg wavelet filtering was used to delineate the threshold curvatures for defining valleys and threshold slope-direction-change for defining the probable channeled portions of the valleys (Lashermes *et al.* 2007), nonlinear diffusion was incorporated to remove noise and to enhance features that are critical for network extraction (Passalacqua *et al.* 2010), a robust two-parameter method was employed to extract drainage networks (Pelletier 2013), and local topographic curvature and *k*-means clustering of contours were utilized to extract valley and channel networks (Hooshyar *et al.* 2016). However, it is important to note that RSG-based methods can be sensitive to DEM errors (Koenders *et al.* 2014).

Considering accuracy and practicality, the extraction of topographic feature lines from contours is important because such an extraction is the first-hand mapping data obtained from field survey or indoor mapping. However, the DEMs of RSG or TIN are normally converted from dense mass information (on contours, the 'infinitely dense' points are identified) to less dense landform information of point sets, with larger intervals. Moreover, the amount of information is decreased. There are two types of methods used for extracting topographic feature lines based on contours, ie single points and point groups for tracing. The first type includes the methods based on the Douglas–Peucker algorithm or TIN. Jin and Gao (2005) first used the Douglas–Peucker algorithm to extract one topographic feature point for the contours. Although the extracted results of the feature points were well in the whole, the traced topographic feature lines were generally too stiff because only one straight line connected two adjacent contours (without other choices) regardless of how large the deflection angle was and whether spatial logical conflicts existed. In this study, the so called spatial logic conflicts refer to the cases where the topographic feature lines do not intersect with the contours (completely or orthogonally); the conflicts can also refer to the

negative topographic feature lines from the 'upstream' to 'downstream' (some places can be found as partially 'climbing the slope' as well). Furthermore, if the tracing directions on the sparsely spaced neighboring contours differ greatly, the topological relationships between the traced topographic feature lines and the contours may be destroyed. Regarding the methods based on TIN, Ai (2007) used the Delaunay triangulation in the bending depth expression of single contours to recognize the hierarchical structure and extract the drainage system of the study area. Based on this method, Zheng *et al.* (2015) used discrete curve evolution (DCE) to dynamically segment the contours into geometric/valley bends and detect the valley feature points with respect to the noise and distortion of contours and found that the extracted Voronoi skeletons from the Delaunay triangulation built from the contours could distill accurate channel paths in the complex terrain. However, the topographic gradient was not included by this connection method. As for the second type, Xiong and Li (2015) employed the mean shift (Fukunaga and Hostetler 1975) idea to find the topographic feature points that have the maximum probability for flow direction by implementing a multifactor watercourse model to extract ridge and valley lines. Different from the first three methods, this method particularly starts from a chosen topographic feature point to link it to an optimal feature point (among the feature point groups) on the neighboring contour. The extraction results were better, but no consideration was made for the process of generating valley and ridge lines along the directions of gentle slopes.

This study introduces new approaches to extract more complete, accurate and natural topographic feature lines from contours on different topographic gradients. Three contributions of our paper are as follows: (1) structure trees of feature point groups are established. Relying on the stack technique, the completeness of tracing topographic feature lines is ensured. (2) We have not only put forward the mathematical model used to trace optimal points from feature point groups along the directions of steep slopes, but also the convergent searching algorithm to determine the best position when generating topographic feature lines along the directions of gentle slopes. (3) To reduce the spatial logical conflicts between the extracted topographic feature lines and contours as much as possible, this paper presents that these two kinds of lines should intersect orthogonally at the intersection points.

The remainder of this paper is organized as follows. [Section 2](#) introduces methods of extracting topographic feature lines on the basis of valley point groups, ridge point groups and their filtration, and mountain tops and saddle points, with their 3D coordinates automatically calculated on the basis of nearby contours. [Section 2](#) explains how to build structure trees for the feature point groups and how to trace the topographic feature lines using multi-criterion methods and giving consideration to the different topographic gradients. [Section 3](#) displays the experimental results of this paper and indicates advantages of our new method through comparison with other known methods, [Section 4](#) provides a discussion based on the results of this study and [Section 5](#) offers the conclusions of our work and points out the scope of future research with respect to the integrated generalization of contours and river systems.

## 2. Methodology

The framework for extracting topographic feature lines from contours on different topographic gradients is shown in Figure 1. We first group the negative and positive feature points, and extract mountain tops, hollow bottom points and saddle points from contours. Then, we build structure trees for these feature point groups and recognize the ‘mainstreams’ and ‘tributaries’ of the structure trees. Afterwards, we put forward multi-criterion methods containing the proposed mathematical model and convergent searching algorithm for best position to extract topographic feature lines along the directions of steep as well as gentle slopes, respectively. Finally, the hierarchical structure of the topographic feature lines was established.

### 2.1. Feature point groups: definition and filtration

In order to establish the spatial relationships among the contours, and to obtain the accurate topographic feature points calculated from contours, we need first detect and adjust the directions of source contours as required. For this purpose, the principle considered is ‘left higher, right lower,’ which means that along the digitizing direction of a contour, the elevation of any point near the left side of the contour is

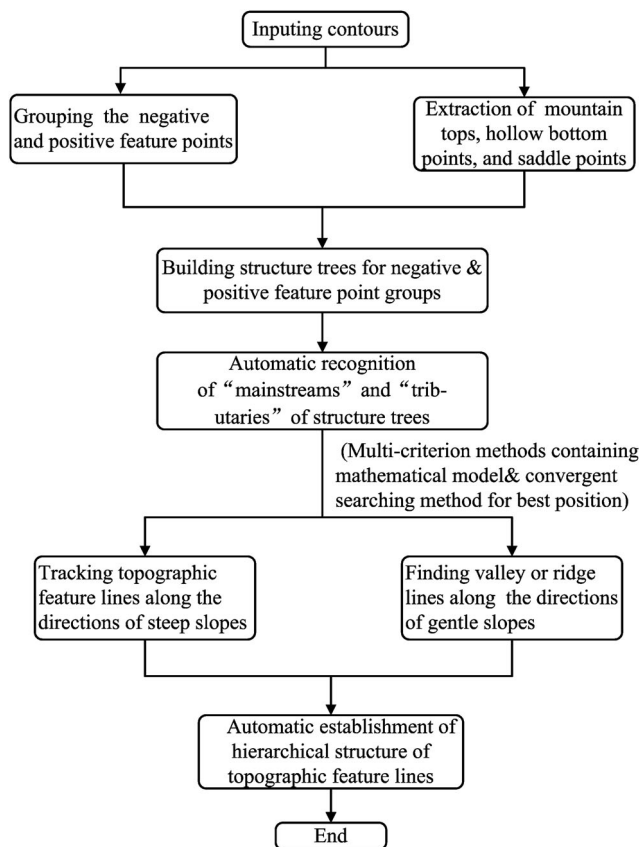


**Figure 1.** Workflow implemented for extracting topographic feature lines.

higher than the elevation of the contour itself, whereas the elevation of any point near the right side of the contour is lower than the elevation of the contour itself. Second, we construct the spatial relationships among the contours, ie contour trees. There are various methods to build the contour trees (Qiao *et al.* 2005, Guilbert 2013, Xiong and Li 2015). Since this is not the focus of this article, we employ directly the method presented by Xiong and Li (2015) to build the contour trees. Finally, we extract valley points and ridge points, as well as the mountain tops, hollow bottom points and saddle points later.

In this paper, the definition of curvature (Freeman and Davis 1977)  $k_Q$  can be expressed as follows (Figure 2):

$$k_Q = \lim_{P \rightarrow Q} \frac{d\alpha}{\overline{PQ}} \approx \frac{\Delta\alpha}{\overline{PQ}} \quad (1)$$

The curvature  $k_Q$  at point  $Q$  can also be written as follows:

$$k_Q = \lim_{M \rightarrow Q} \frac{d\beta}{\overline{MQ}} \approx \frac{\Delta\beta}{\overline{MQ}} \quad (2)$$

Considering the possible large difference in the distance between  $\overline{MQ}$  and  $\overline{QP}$ , removing any of the segments as the denominator may affect the precision of the calculated curvature. Therefore, we preferred using the approximate mean curvature calculated equation given below:

$$k_Q \approx \frac{(\Delta\alpha + \Delta\beta)/2}{(\overline{MQ} + \overline{QP})/2} = \frac{(\Delta\alpha + \Delta\beta)}{(\overline{MQ} + \overline{QP})} \quad (3)$$

Thus, the approximate mean curvature value at point  $Q$  as well as other points can be calculated (Figure 2).

In Equations (1) and (2),  $\Delta\alpha$  and  $\Delta\beta$  are the deflection angles at points  $P$  and  $M$ , respectively, the units of deflection angles and lengths are radian (rad) and meter (m). The feature points on the valley and ridge lines can be extracted by setting suitable curvature thresholds.

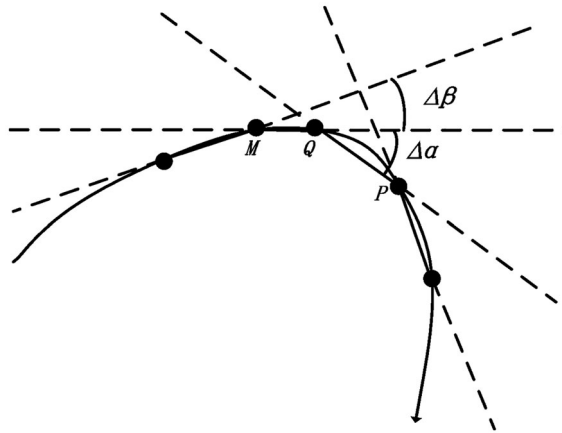


**Figure 2.** Calculation of approximate mean curvature value at point  $Q$ .

Then, we defined a feature point group as a set of neighboring topographic feature points on contours, with small distances and definite uniform curvature sign. Some isolated points that had little impact were excluded. Simultaneously, a small number of points whose absolute curvature values are smaller than a threshold are considered as the 'demarcation' of the two feature point groups. If the distance of the two feature point groups near the 'demarcation' is considerably large, these two feature point groups cannot be merged; otherwise, the feature point groups on both sides of the 'demarcation' are merged. Nevertheless, certain 'unimportant' feature point groups may still exist. In this situation, the DCE method can be used to deal with these 'unimportant' feature point groups, because it can eliminate noise and obtain the best feature points from contours (Bai *et al.* 2007). The decision to reserve the joint point of line segments  $S_i$  and  $S_{i+1}$  is dependent on the important indices, which can be calculated as follows:

$$K(S_i, S_{i+1}) = \frac{\beta(S_i, S_{i+1})L(S_i)L(S_{i+1})}{L(S_i) + L(S_{i+1})} \quad (4)$$

where  $\beta(S_i, S_{i+1})$  is the turning angle at the common vertex of segments  $S_i$  and  $S_{i+1}$ ; and  $L(S_i)$  and  $L(S_{i+1})$  represent the lengths of  $S_i$  and  $S_{i+1}$ , respectively. A higher  $K(S_i, S_{i+1})$  indicates a greater contribution of the common point of  $S_i$  and  $S_{i+1}$  to the shape. Feature point groups should be effectively and suitably removed or reserved in accordance with different landforms.

## 2.2. Mountain top and saddle point extraction

### 2.2.1. Extraction method of mountain tops and hollow bottom points

Generally, if the measured position and elevation of mountain tops already exist in the contour source data, then such position and mountain tops can be used directly. However, this is normally not the case. The extraction of the approximate position and elevation of the mountain tops completely based on the contours is described as follows (Figure 3).

1. As shown in Figure 3(a), the local highest closed contour 2 was rasterized subtly to extract the approximate mountain top  $O$  using a peeling algorithm (Petitjean and

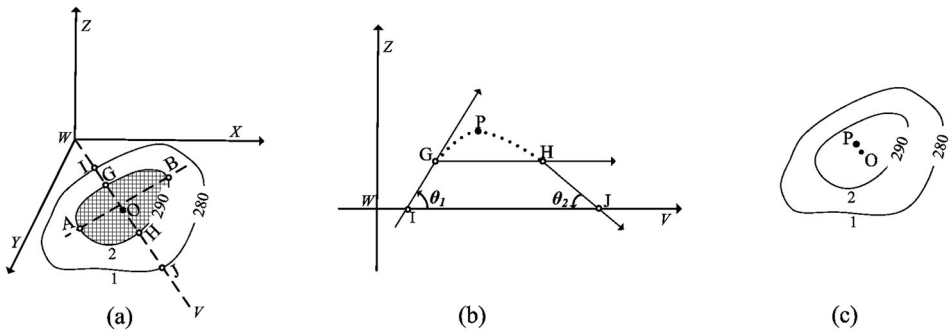


**Figure 3.** Extraction of mountain tops. (a) Choosing location and direction of section line in 3D coordinate system WXYZ. (b) Calculating approximate location and elevation of mountain top  $P$  by profile line  $IGPHJ$  using improved Akima algorithm in profile  $WZV$ . (c) According to nearby landform, more accurate position of mountain top should be point  $P$  rather than point  $O$ .

Saporta 1992). Then, a line  $AB$  was taken as the main direction with vertices  $A$  and  $B$  from the polygon of contour 2 because this line has the longest distance than any other two vertex combinations in this contour. After that, a vertical profile was made through point  $O$ , with the direction perpendicular to line  $AB$  in the 3D coordinate system  $WXYZ$ .

2. As shown in Figure 3(b), a 2D coordinate system  $ZWV$  is formed. Then an improved Akima algorithm (Xu *et al.* 1993) which originated from the Akima algorithm (Akima 1970) was used, because the improved Akima algorithm has certain advantages over the original. These include faster calculation speed, more symmetrical shape of the interpolated curve on both sides of the central point, controllable tightness of the curve and increased adaptability in automated cartography. Based on the improved Akima algorithm and the angles of  $\theta_1$  and  $\theta_2$ , a cross-section curve  $\widehat{GH}$ , on which the vertex  $P$  (with the local highest elevation of 296.3 m) can be seen as the mountain top, is attained.
3. In Figure 3(c), you can see that the elevation of the mountain top is higher than that of contour 2 by 6.3 m. During the calculation, the elevation of the mountain top cannot exceed that of the nearest closed contour over one elevation interval (10 m in this example). In the current article, the elevation values of mountain tops are expressed by only one digit behind the decimal point because of their limited accuracy (from estimation and not surveyed results). Such presentations are also used for saddle points.
4. The extraction of the position and elevation of hollow bottom points is similar, but upside down, to the extraction of mountain tops.

### 2.2.2. Convergent searching algorithm for best position and extraction of saddle points

In order to extract saddle points, we present a convergent searching algorithm for best position. Moreover, it plays a vital role in extracting topographic feature lines along the directions of gentle slopes later.

**2.2.2.1. Convergent searching algorithm for best position.** The best position means an ideal position satisfying certain mathematical conditions. The convergent searching algorithm described here is a convergent process to find the best position through the purposeful adjustment of the changing directions and angles of subsequent searching steps.

Taking the contour of a valley as an example (Figure 4(a)). A determined feature point  $S_0$  was used first to generate a downward short line segment  $S_0S_1$  perpendicular to a tangential line  $T$  passing through  $S_0$ , and the point  $S_1$  was the best end position. Next, the trial 1st step was carried out along the direction of the line  $S_0S_1$ . With respect to the comparison of the current distance (eg the shortest distance from the best position to the respective contour on both sides) difference between  $LP$  and  $RP$ , if the position cannot meet the mathematical condition, the 2nd step is formed with angle  $\beta$  toward the left side because  $|LP| > |RP|$ . Then, we observed if the current searching manner has a better result than obtained by the 1st step. If yes, the current angle and direction of the searching manner was continued. Otherwise, a 3rd step was formed with halved angle ( $\beta/2$ ) and reverse



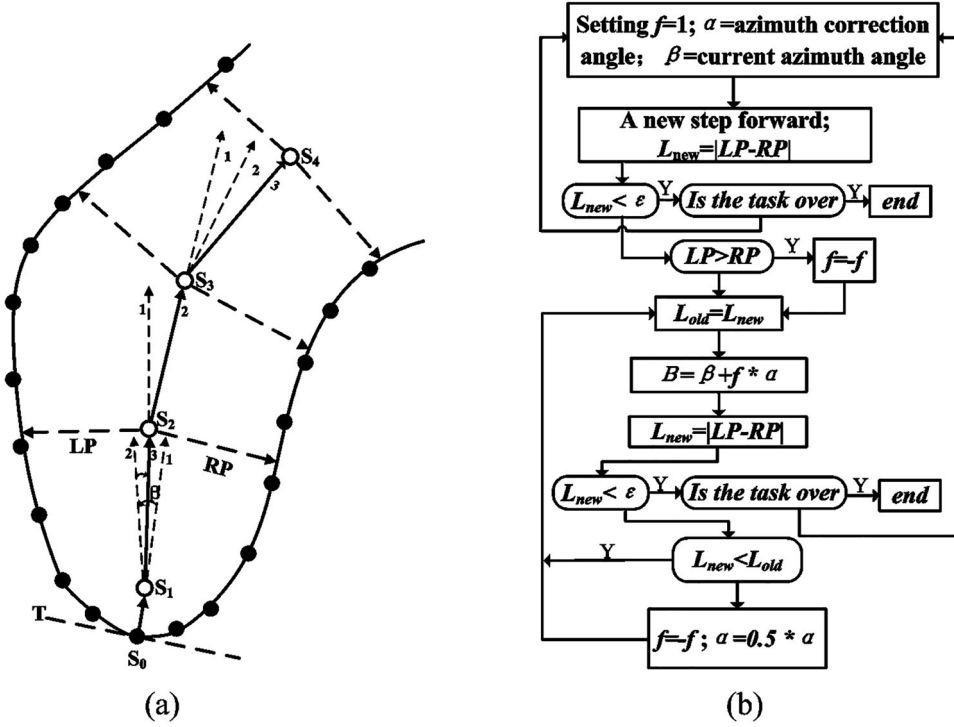


**Figure 4.** Searching with alternative directions and halved angles. (a) Sketch of midline generation; (b) flowchart of convergent searching for best position by using generation of midline as an example.

direction. Thus, the best position was found quickly. Finally, a median line (the solid line  $S_0S_1S_2S_3S_4$ ) was generated for the valley. The concrete search process with reverse direction and halved angle is shown in Figure 4(b), in which  $f$  (flag that records whether the current direction needs to be reversed),  $\alpha$  (azimuth correction angle) and  $\beta$  (current azimuth angle) are initialized variables. In addition, the  $L_{new}=|LP - RP| < \varepsilon$  is the mathematical condition used to end the procedure of one searching step.

**2.2.2.2. Extraction of saddle points.** Based on the spatial relationship between contours, a saddle point should exist between contours  $C_1$  and  $C_2$ , which have a ‘sibling’ relationship (Figure 5(a)). The concrete process is described as follows.

1. As shown in Figure 5(a), two positive feature points with the shortest distance between contours  $C_1$  and  $C_2$ , such as points  $A$  and  $B$ , were found. We used the best position convergent searching algorithm (Section 2.2.2.1) to obtain the median line  $\widehat{AB}$  in the saddle area.
2. The sums of the shortest distances between  $\widehat{AB}$  and the two opposite neighbouring contour parts, both of which belonged to the ‘parent’ of  $C_1$  and  $C_2$  topologically, were calculated for each vertex on curve  $\widehat{AB}$  with small intervals. At last, the vertex  $C$  was selected as the candidate saddle point because it has the minimum value of the distance sums (Figure 5(b)).

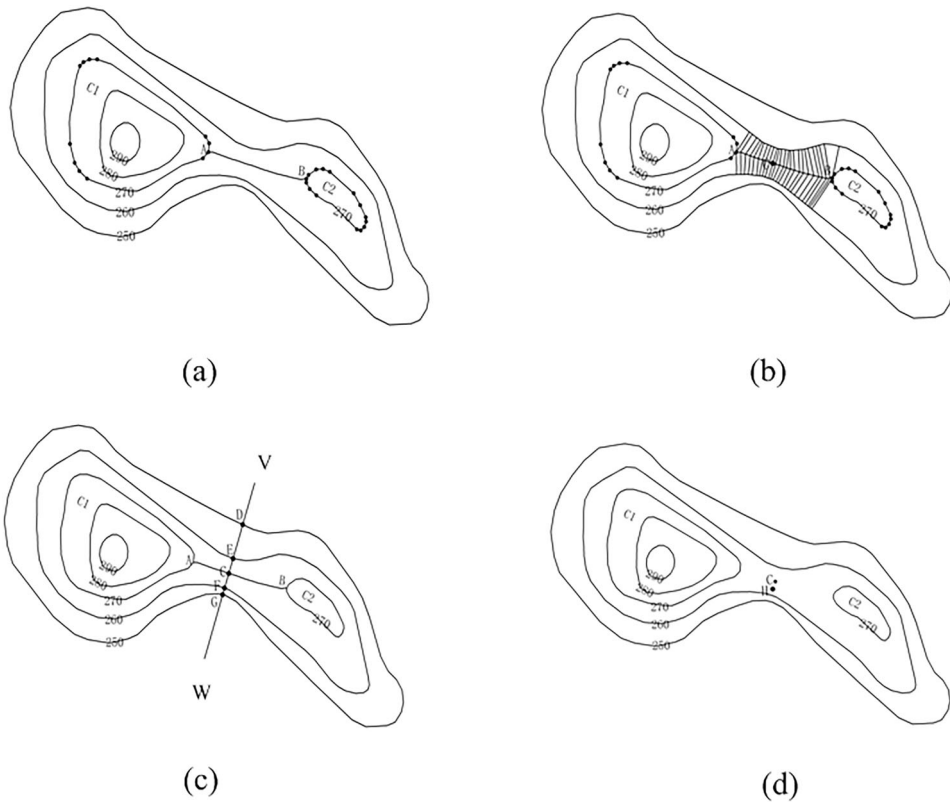


**Figure 5.** Extraction of saddle points. (a) Formation of smoothed line from point A to B, on contours  $C_1$  and  $C_2$ , respectively. (b) Regulation of trajectory of  $\widehat{AB}$  to form a midline from A to B to parent contour of  $C_1$  and  $C_2$  and determination of point C with the smallest distance sum on curve  $\widehat{AB}$  as the original saddle point. (c) Determination of profile line. (d) Substitution of point C with H to heighten the accuracy of position and elevation of saddle point.

3. An angle bisector line CV through vertex C was constructed by point C and its neighboring two points before and after, and an angle bisector line CW was built in the reverse direction using the same method. Thus, a complete straight line WCV intersected with the neighboring contours in a saddle area at points G, F, E and D (Figure 5(c)).
4. Similar to Section 2.2.1, a profile line with the contours was made to form the curve  $\widehat{FHE}$ . The adjusted position of the saddle point H and its elevation were calculated using the improved Akima algorithm (Xu et al. 1993) (Figure 5(d)).

## 2.3. Using multi-criterion methods to extract topographic feature lines from contours on different topographic gradients

### 2.3.1. Structure trees of feature point groups

As discussed in Section 2.1, the approximate mean curvature values (with correct positive or negative topographic feature signs of all points) can be calculated from the contours. In addition, a concept of feature point groups is defined, and the contour

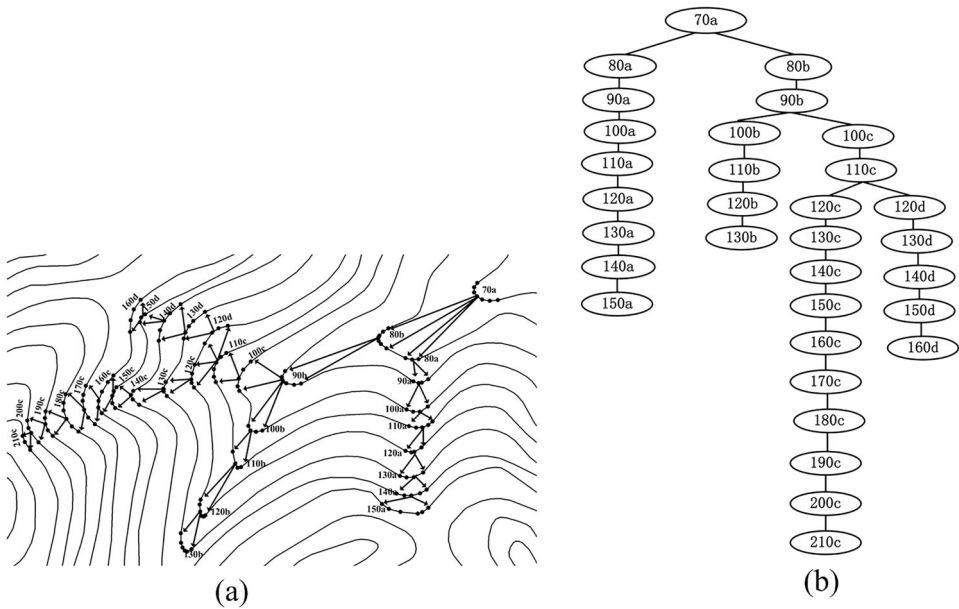


**Figure 6.** Construction of structure tree aiming at feature point groups. (a) Searching process by using scanning method. (b) Structure tree built for feature point groups.

trees are constructed. In this section, we use each feature point group with a negative sign as a node to construct topological trees before tracking topographic feature lines. The tracking principle of positive topographic feature lines is similar.

First, all feature point groups with negative signs were extracted from contours having a suitable threshold value (Figure 6(a)). The feature point groups were named, such as 80a and 80b (80a is the name of the first found feature point group located on a contour with an elevation of 80 m, and 80b has similar explanation). Moreover, the first and end points of each feature point group were recorded. Second, a point from each feature point group, which was the closest to the center of the curve, was selected, and this point was roughly referred to as the representative point of the feature point group. We divided the task of tracking the feature point groups into two stages:

1. For example, the entire contours were scanned in a clockwise manner starting from the smallest elevation (Figure 6(a)), and only one feature point group 70a was found on the contour. Next, the representative point in the feature point group 70a was selected, and the normal vector through this point was calculated, followed by stretching two searching rays upward (forming a 'starting visual angle'), which could be automatically adjusted. The normal vector was taken as the axis of symmetry, then the two searching rays intersected the neighboring contour with an elevation of 80 m to roughly trace the feature point groups upwards.
2. After an overall scanning on the contour (from the next smallest elevation) in the clockwise direction, we found two feature point groups, 80a and 80b (either at least one change of the feature sign or one distance longer than the threshold

existing between the two feature point groups) on this contour at an elevation of 80 m. In the range of intersections between the 'starting visual angle' rays and the neighboring contour with a higher elevation interval, if more than one entire and/or partial point sets of different feature point groups were found, the relevant whole feature point groups could be traced, and a bifurcation from the traced result was formed. These relationships were recorded and roughly traced clockwise using the stack technique until all the feature point groups were traced and the corresponding structure tree of the feature point groups were completely built (Figure 6(b)).

### 2.3.2. Automatic recognition of 'mainstreams' and 'tributaries' of structure trees

For the multi-scale generalization of contours, defining the 'mainstreams' and their 'tributaries' in different classes for topographic feature lines is necessary. Taking a river system as an example, the mainstream is the longest watercourse that contains the highest water yield than other watercourses. The rivers that directly flow into the mainstreams are called the first-class tributaries, and the rivers that directly flow into the first-class tributaries are referred to as the second-class tributaries. However, the limited source data are usually insufficient for the automatic recognition of mainstreams and tributaries according to the abovementioned definition.

Nevertheless, for this purpose, can we be enlightened through the observation of many phenomena in natural geography? In a drainage basin system, which is subject to rainfall or ice/snow melting, the tributaries normally have lesser discharge but higher velocity, and the mainstream normally has higher discharge, but lower velocity. Therefore, the slopes on mainstreams are normally gentler than tributaries. During the dry season, the tributaries normally tend to dry up first, whereas mainstreams normally tend to maintain their characteristic of being perennial rivers as durable as possible. These phenomena may also be used to automatically recognize the 'mainstreams' and 'tributaries' in the hierarchical structure of positive and negative topographic feature lines. According to the topological relationship of the structure tree in Figure 6(b), starting from the root node and ending at the leaf node, the average slope of each path can be calculated as follows:

$$Slope_{ave} = (H_{leaf} - H_{root}) / \sum_{i=1}^{n-1} L_i L_{i+1} \quad (5)$$

where  $\sum_{i=1}^{n-1} L_i L_{i+1}$  refers to valley line's 2D length calculated from the root node to the leaf node using the convergent searching algorithm (Section 2.2.2.1),  $H_{leaf}$  and  $H_{root}$  are the elevations of the leaf and root nodes, respectively. The negative topographic feature line having the smallest average slope in a topological tree is considered to be the 'mainstream', and the rest of the 'rivers' that directly flow into the 'mainstream' are considered to be 'first-class tributaries'. The method for extracting 'second-class tributaries' and so on is similar.

### 2.3.3. Tracking topographic feature lines along the directions of steep slopes

In a section of a wide valley along the directions of steep slopes (Figure 7), for tracing the topographic feature lines, the concrete equation and parameters for calculating

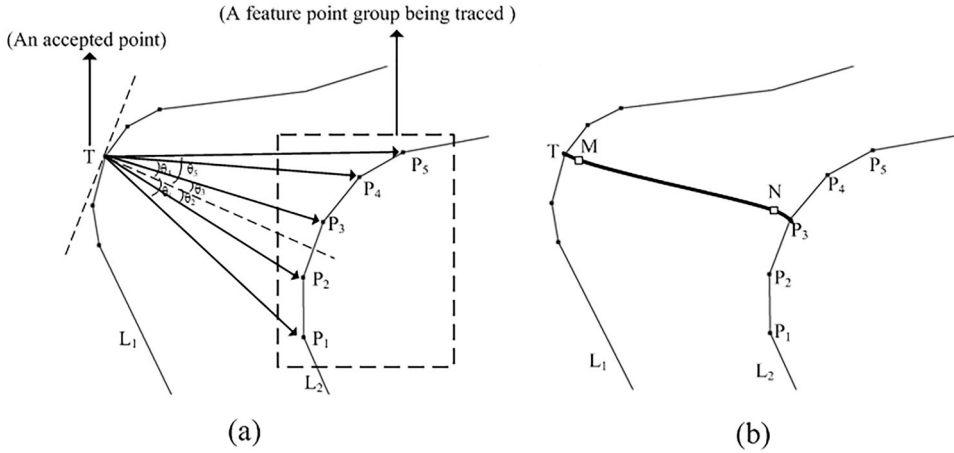


**Figure 7.** Tracking topographic feature lines along the directions of steep slopes. (a) Determination of target feature point using multiple criteria;  $T$  is an accepted point on  $L_1$ , which has higher elevation than  $L_2$ . The five points ( $P_1, P_2, P_3, P_4$  and  $P_5$ ) are made up of feature point group being traced, in which an optimal point should be chosen in accordance with four weight coefficients in Table 1. (b) Generation of stretch of topographic feature line perpendicular to contours  $L_1$  and  $L_2$ .

the ‘attraction’ of each point in a feature point group being traced are expressed in Equation (6), Table 1 and Figure 7. According to the cartographical requirements, the selection of topographic feature points on neighboring contours can be determined by the sum of the following four criteria: (1) value of the curvature, (2) Euclidean distance, (3) deflection angle and (4) middleness value. Here, we refer to the point with the biggest sum in Equation (6) as the point with the greatest ‘attraction’ to be traced.

$$Mp(x) = k_1 * \left( \frac{|C_x|}{M_1} \right) + k_2 * \left( 1 - \frac{S_x}{M_2} \right) + k_3 * \left( 1 - \frac{|\theta_x|}{M_3} \right) + k_4 * \left( 1 - \frac{abs(L_{mid} - \sum_{i=1}^x |P_{i-1}P_i|)}{L_{mid}} \right), \quad (6)$$

$$x = 1, 2, 3 \dots n$$

where  $M_1 = \max|C_x|$ ,  $M_2 = \max|S_x|$ ,  $M_3 = \max|\theta_x|$  and  $n$  is the total number of points in the feature point groups being traced; when  $x = 1$ , let  $P_0 = P_1$ , and  $k_4 = 0$ .

For example, negative feature point groups were identified on contours  $L_1$  and  $L_2$  (Figure 7(a)). No Euclidean distance and deflection angle existed because the feature point group on contour  $L_1$  was the beginning, and only curvature and middleness were taken into consideration. In this condition, let  $k_2 = 0$ ,  $k_3 = 0$ ,  $k_1 + k_4 = 1$  for calculation, so point  $T$  was the only selected feature point according to Equation (6) on the contour  $L_1$ . Points  $P_1, P_2, P_3, P_4$  and  $P_5$  were feature points being traced on contour  $L_2$ , the absolute curvature value of point  $P_3$  was the largest (Equation (3)) and the closest point to the middle position. Therefore, the ‘attraction’ of point  $P_3$  on contour  $L_2$  was the largest, and  $P_3$  was traced. The concrete ‘attraction’ of  $P_3$  can be calculated using Equation (6). Finally, a topographic feature line segment from point  $T$  to point  $P_3$  using improved Akima algorithm (Xu *et al.* 1993) was attained. Simultaneously, with the help

**Table 1.** Parameters and their description.

Parameters	Description
$M_p(x)$	The 'attraction' of each point in the feature point group being traced
$k_i$ ( $1 \leq i \leq 4$ )	Weight coefficient of each criterion ( $0 \leq k_i \leq 1$ , $\sum_{i=1}^4 k_i = 1$ )
$C_x$	Curvature of each point in the feature point group being traced
$S_x$	Euclidean distance between an accepted feature point and each point in the feature point group being traced
$\theta_x$	Deflection angle between previous and ongoing tracing directions
$L_{\text{mid}}$	$L_{\text{mid}} = (\sum_{i=1}^n  P_{i-1}P_i )/2$ , half length of the feature point group being traced

of points  $M$  and  $N$ , correct intersection relationships were found using angular bisectors  $\overline{TM}$  and  $\overline{NP}_3$  to simulate the perpendicular relationship between the curve  $\widehat{TP}_3$  and the contours  $L_1$  and  $L_2$ , ie  $\overline{TM} \perp L_1$  and  $\overline{NP}_3 \perp L_2$  (Figure 7(b)).

In this article, three reasons were identified to set the four criteria. Geomorphology and hydrology have influenced each other since antiquity. Thus, inferring the shapes of negative topographic feature lines on the basis of contours and the characteristics of channelized paths is possible. If a set of contours are relatively dense, and the first topographic feature point  $T$  on contour  $L_1$  has been accepted (Figure 7), the next point to choose for tracing the topographic feature line on the topographic feature point group of the adjacent lower contour  $L_2$  will have a different 'attraction' to the river path coming from point  $T$ . First, when a negative topographic feature line is formed passing over neighboring contours, it should choose the point with the maximum curvature value on the contour. Second, the tracing step from the starting to end points should have the shortest Euclidean distance due to the densely distributed neighboring contours. Third, the deflection angle in tracing a new point on the next contour should be best near  $0^\circ$ . Finally, the fourth requirement in tracing the topographic feature line is to choose the middle point of the feature point group on the adjacent contour. The joint working fashion in this study is designed using the four criteria and their respective weight coefficients to keep the tracking result more stable.

#### 2.3.4. Finding valley or ridge lines along directions of gentle slopes

Only when narrow valley or ridge terrains are detected, can the algorithm for extracting topographic feature lines that will be introduced as follows more subtly be performed. Before introducing this algorithm, let us describe, for example, how a virtual valley line is formed step-by-step between at least two contours on each side of a valley. As shown in Figure 8(a), taking a sharp U-turn, contour  $L_1$  is cut by a part of a line on the map as the first layer of the contour polygon, which is nearest to the virtual valley. If the two ends of this U-turn contour intersect the neat line of the map on point  $B_1$  and  $B_2$  and the chosen optimal negative feature point on contour  $L_1$  is point  $A$ , then,  $B_1AB_2B_1$  is a polygon, which can be referred to as a closed contour polygon. A definition is given for 'thin degree' (TD) by the aforementioned polygon:  $TD = (\text{perimeter of the contour polygon}) / (\text{area of the contour polygon})$ . If  $TD \geq ES$  (threshold for an elongated shape), this polygon is referred to as an elongated polygon. Although the extraction of valley lines is considered as an example, the same principle is used for the ridge lines. If two elongated neighboring contour polygons are detected, two steps are taken to generate the valley or ridge lines as follows:

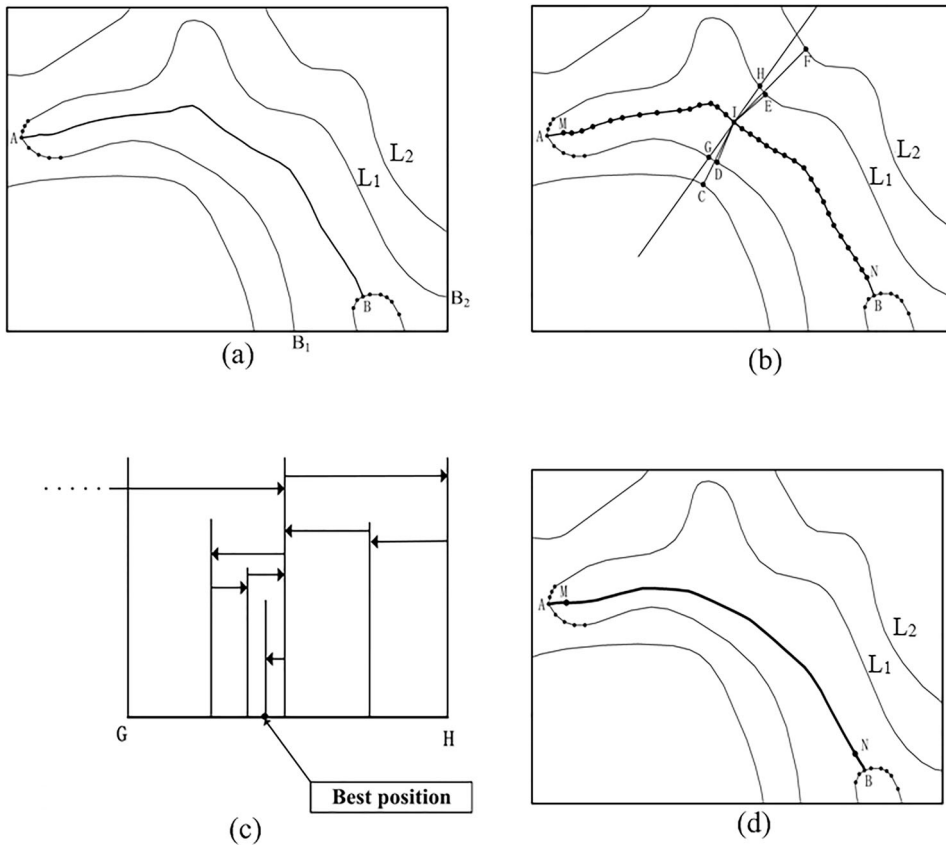


**Figure 8.** Tracking of valley lines in gentle slope region. (a) Construction of closed contour polygon  $B_1AB_2 B_1$  and midline  $\widehat{AB}$ . (b) Regulation of midline  $\widehat{AB}$  point by point by using formula (7). (c) Illustration of convergent searching algorithm to determine best position. (d) Determined valley line with high accuracy (black line in boldface).

1. According to the convergent searching algorithm for best position (Section 2.2.2.1 and Figure 4), a midline with a length (eg 10 m) is generated (Figure 8(a)).
2. The first point of the midline is point  $M$ , then starting from the second point on the midline, a series of points should be regulated individually to subtly regulate the positions of the imaginary valley line points according to the slopes on each side of the valley line (Figure 8(b)). For each point (ie point  $I$  in Figure 8(b)) on the midline, four points more, ie  $C, D, E$  and  $F$ , can be found because such points and point  $I$  constitute the four shortest distances to the roundabout contours  $L_1$  and  $L_2$  nearby. In this way, the extraction of topographic feature lines can depend on more local geomorphological information. For example, the position of point  $I$  can be regulated on the midline once again using the convergent searching algorithm for best position according to the criterion equation:



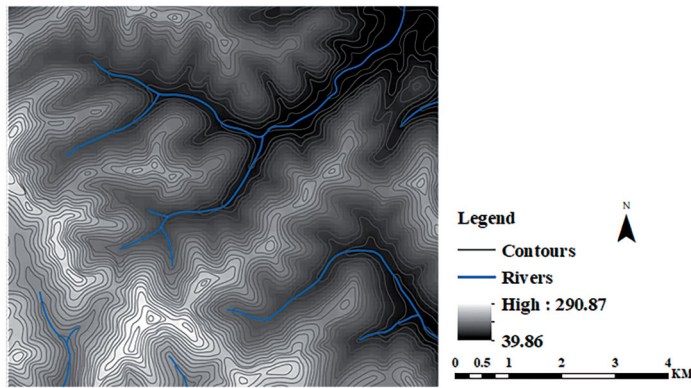


**Figure 9.** DEM with a resolution of 25 m, contours and rivers.

$$\frac{\sqrt{\overline{ID}}}{\sqrt{\overline{IC}}} \approx \frac{\sqrt{\overline{IE}}}{\sqrt{\overline{IF}}} \quad (7)$$

The convergent process (Fei 2002) can be seen in Figure 8(c). Starting from point *I*, a step forward along the line  $\overline{GH}$  (with a suitable length, eg 1 m) is made to test and regulate a point position until the best position is found using the convergent searching algorithm (Section 2.2.2.1 and Figure 4(b)).

Four mathematical square root symbols were used in this study because the further a contour is located, the less impact the contour can exert on the location of the imaginary valley line. However, the actual micro-regulation of the trajectory of point *I* was along the straight line  $\overline{GH}$ . After the point *I* was repositioned, the new positions (*C*, *D*, *E* and *F*) and new distances ( $\overline{IC}$ ,  $\overline{ID}$ ,  $\overline{IE}$  and  $\overline{IF}$ ) were recalculated. In this way, when regulating the point *N*, we can use Equation (6) to trace optimal point (eg point *B*) from the feature point group on the neighboring contour, no deflection angle existed because point *N* is not on the contour. After all the points on the primary mid-line were regulated, we attained the negative topographic feature line with high accuracy (Figure 8(d)).

### 3. Experimental results and comparison

#### 3.1. Data source

In this paper, the experiment area is located in the southern area with abundant precipitation in Anhui province, China. The data include DEM with a resolution of 25 m, contours with a maximum elevation value of 290 m, a minimum elevation value of 40 m and a contour interval of 10 m, and rivers (scale 1:50,000) (Figure 9). We first use the contours to extract topographic feature lines, then the rivers in the same area were utilized to evaluate the extracted partial negative topographic feature lines in a proper way to indirectly show the accuracy of the extracted topographic feature lines, and the DEM with a resolution of 25 m in the same area was employed to make comparison with our methods.



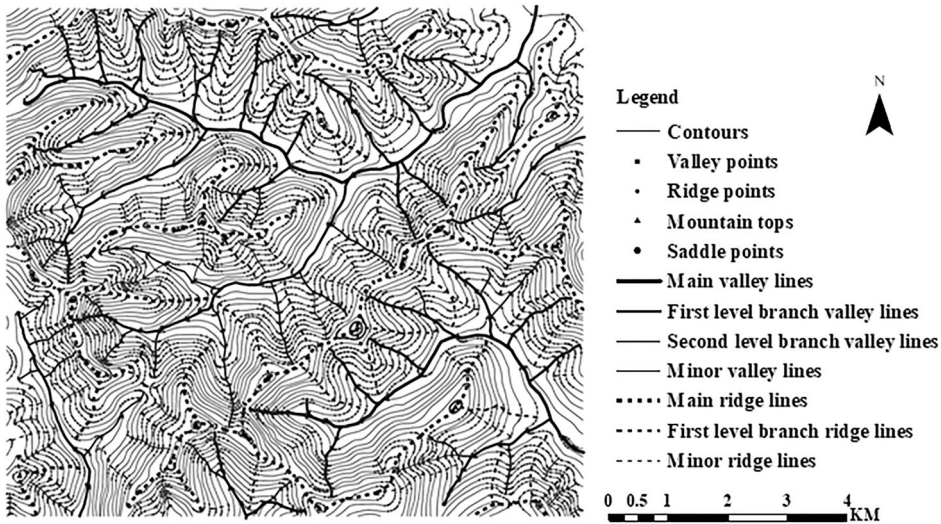


Figure 10. Final extraction result of topographic feature lines.

### 3.2. Experiments with contours

Besides the usage of the convergent searching algorithm, the quality of topographic feature line extraction is affected by four criteria ( $C$ ,  $S$ ,  $\theta$ ,  $L_{mid}$ ) and their weight coefficients ( $k_1$ ,  $k_2$ ,  $k_3$  and  $k_4$ ;  $0 \leq k_i \leq 1$ , and  $\sum_{i=1}^4 k_i = 1$ ) according to Equation (6) in Section 2.3.3 to a large extent.

Therefore, we need to set reasonable values for the four weight coefficients. In this study, we regard the four weight coefficients as temporary free variates in turn, and the interval of each variate is set to be 0.05. For example,  $k_i = \{0, 0.05, 0.1, 0.15, \dots, 1\}$  ( $i = 1, 2, 3$  and  $4$ ). In all mathematical combinations, the sum of the four weight coefficients must be 1, ie  $\sum_{i=1}^4 k_i = 1$ . Finally, through experiments, it was concluded that when  $k_1 = 0.1$ ,  $k_2 = 0.8$ ,  $k_3 = 0.05$  and  $k_4 = 0.05$ , the topographic feature lines with hierarchical characteristics can be extracted in a quite satisfactory way for this experimental area (Figure 10).

### 3.3. Comparison with RSG-based and Voronoi skeleton-based methods

There are various methods to extract topographic feature lines based on a RSG-type DEM with their own characteristics, such as D8 algorithm (O'Callaghan and Mark 1984) and morphology-based algorithm (Molloy and Stepinski 2007). Due to the space limitation of this article, we cannot portray all the extraction results completely. At the same time, some authors have made comparisons for these algorithms (Tarboton *et al.* 1991, Montgomery and Dietrich 1992, Montgomery and Foufoula-Georgiou 1993, Molloy and Stepinski 2007, Jasiewicz and Metz 2011, Zheng *et al.* 2015). Therefore, a mixture of hydrology and morphology-based algorithms, which can overcome some shortcomings compared with others to some extent (Jasiewicz and Metz 2011), was chosen to compare with our method. Figure 11(a) shows the topographic feature lines extracted by Jasiewicz and Metz (J-M method) in the test area, the results are good

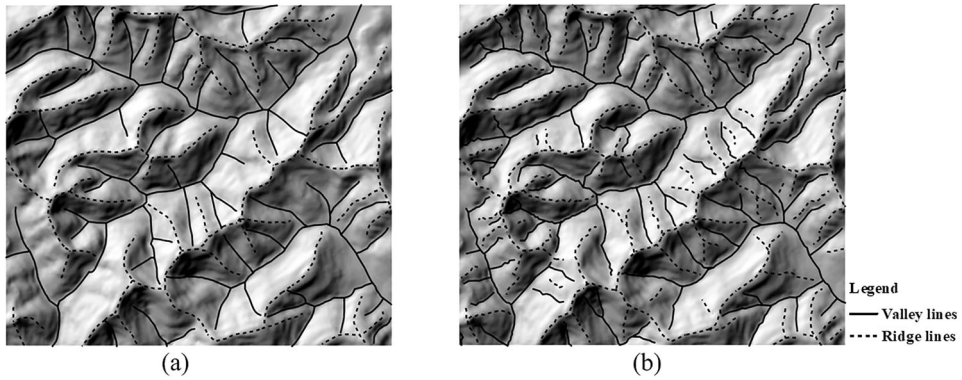


**Figure 11.** Comparison of topographic feature lines delineated by different methods. (a) J–M method with tangential curvature threshold of 0.01 and accumulation threshold of 20. (b) Topographic feature lines generation by the Voronoi skeleton-based method.

enough based on the accuracy of the current DEM with 25 m resolution. Given that the generalization of contours in our future works, we tend to extract more complete, accurate and natural topographic feature lines from contours.

Simultaneously, the Voronoi skeleton-based method of channel network extraction from contours (Zheng *et al.* 2015) was also chosen to compare with our multi-criterion methods. As shown in Figure 11(b) in the same test area, the results are also good, but no consideration was made for possible different gradients on both sides of the valley or ridge regions.

However, a more desirable result is the generation of an accurate topographic feature lines considering the topographic gradients when confronted with a terrain region with complex surface morphology. In general, if there are rivers in the original terrain data, the rivers can be used for evaluation in a proper way.

Therefore, to show the accuracy of the extracted topographic feature lines, we employed a quantitative evaluation method with Equation (8) to compare partial valley lines (only near where there are rivers in Figure 9) in this study, and the average route difference of the extracted topographic feature lines (relative to the existing rivers) were calculated by the following expression:

$$AveRouteDif = \frac{\sum Sli_m}{\sum_i^n L_i} \quad (m = 1, 2, 3 \dots m; i = 1, 2, 3 \dots, n) \quad (8)$$

where *AveRouteDif* (ARD) is the average route difference whose sketching can be shown in Figure 12,  $\sum Sli_m$  is the total difference area of the sliver polygons formed from the overlay of the extracted topographic feature lines and the rivers, *n* is the total number of actual rivers, and *L<sub>i</sub>* is the length of the rivers.

In view of the difference of data type between contours and DEMs, we only compare the average route difference of our methods with that of the Voronoi skeleton-based method only near where there are rivers. Finally, the average route difference of our methods and the Voronoi skeleton-based method are 3.46 m and 4.50 m, respectively. The results indicated that the lower the average route difference, the more the accuracy of the extracted topographic feature lines.

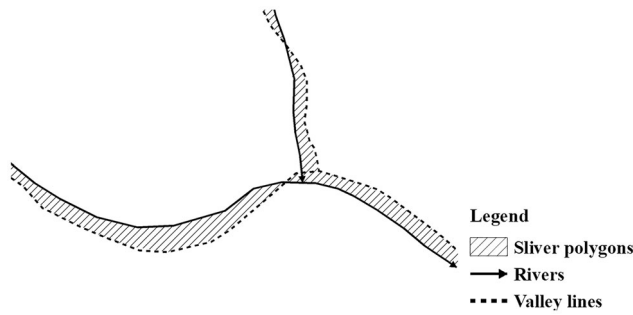


**Figure 12.** Sketching of route difference areas.

#### 4. Discussion

In this study, we have used the mathematical model and the convergent searching algorithm for best position to extract topographic feature lines from contours. In the process of topographic feature line tracing, we have taken different topographic gradients into account on the basis of the nearby contour's feature point groups or the distribution of nearby contours themselves. In addition, the spatial logical conflicts between topographic feature lines and contours are reduced. To compare the accuracy of feature line extraction, we have employed a quantitative evaluation method to compare our results with rivers. The results show that the topographic feature lines extracted by our proposed method can be better than those extracted by the Voronoi skeleton-based method.

Simultaneously, in order to show the generalization ability of the proposed method, we employed another two different regions for experiments as shown in [Figures 13\(a\)](#) and [14\(a\)](#). The data in [Figure 13\(a\)](#) comes from part of Anhui province of China, including DEM with a resolution of 25 m, contours with a maximum elevation value of 600 m, a minimum elevation value of 240 m and a contour interval of 10 m, and rivers (scale 1:50,000). The data in [Figure 14\(a\)](#) show the DEM with a resolution of 5 m, contours with a maximum elevation value of 1085 m, a minimum elevation value of 900 m and a contour interval of 5 m, and rivers (scale 1:10,000) from part of Shaanxi province of China. According to the method of extracting terrain feature lines in [Section 2](#), the calculation method for the four weight coefficients in [Section 3.2](#), as well as the comparison with the RSG-based and Voronoi skeleton-based methods, we respectively obtained the extraction results as shown in [Figure 13\(b–d\)](#) as well as [Figure 14\(b–d\)](#).

Besides, the quantitative evaluation method with [Equation \(8\)](#) to compare partial valley lines (only near where there are rivers) was used to show the accuracy of the extracted topographic feature lines. The results are that the average route difference of our methods and the Voronoi skeleton-based method in [Figure 13\(b,d\)](#) are 4.01 m and 4.65 m, respectively, and that in [Figure 14\(b,d\)](#) are 0.42 m and 1.37 m, respectively.

It is seen from [Figures 13\(c\)](#) and [14\(c\)](#) that the RSG-based method extracts topographic feature lines with good integrity and fewer short branches, but certain challenges still exist for the extraction of high-quality topographic feature lines in high-resolution topographic data, eg the terrain noise cannot be suppressed effectively, the

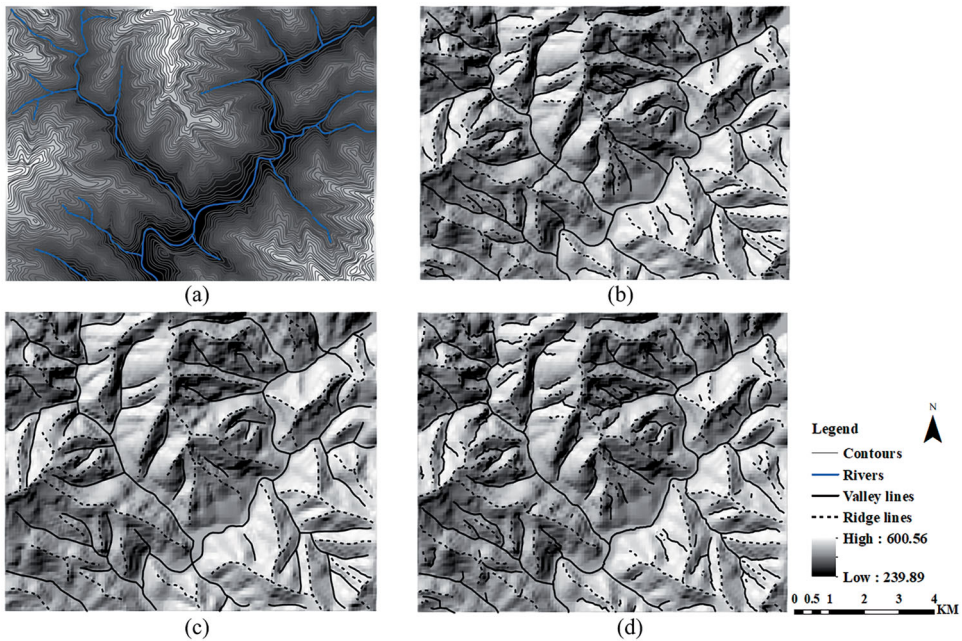


**Figure 13.** Original data from part of Anhui province of China and comparison results with different methods. (a) DEM with a resolution of 25 m, contours, and rivers (scale 1:50,000). (b) The proposed method with  $k_1=0.4$ ,  $k_2=0.45$ ,  $k_3=0.1$  and  $k_4=0.05$ . (c) J–M method with tangential curvature threshold of 0.02 and accumulation threshold of 40. (d) Topographic feature lines generation by the Voronoi skeleton-based method.

threshold of feature point extraction is uncertain, especially the grid size of DEM (which is not easy to determine when digital simulation of flowing water is processed by the J–M method), and some irregular terrains still exist. However, the contours with higher accuracy, and less storage demand are more practical. By using the Voronoi skeleton-based method, the complete topographic feature lines can be extracted in gentle-slope areas. However, the topographic gradient is not taken into consideration. In this paper, we have used the rivers for evaluating the precision of the extracted topographic feature lines (only near where there are rivers), because geomorphology and rivers in nature are mutually constrained and affected in theory, the extracted valley lines should overlap with or be close to the rivers as much as possible; but the Voronoi skeleton-based method fails to consider this situation. Furthermore, the topographic feature lines with complete extraction, higher precision and hierarchical characteristics are significant for our future works. If our task is the integrated generalization of contours and river systems, enough vector contours with higher accuracy should be used as the source data, and important but implicit topographic feature lines should be extracted from the original contours as necessary (as implemented in manual cartography). The extracted results based on the RSG-type DEM and Voronoi skeleton methods do not satisfy these demands easily.

There are two limitations of this study. First, it is necessary to obtain sufficient and meaningful feature points of micro-geomorphology according to visual and empirical judgment to construct feature point groups. If we keep too many feature points, it is



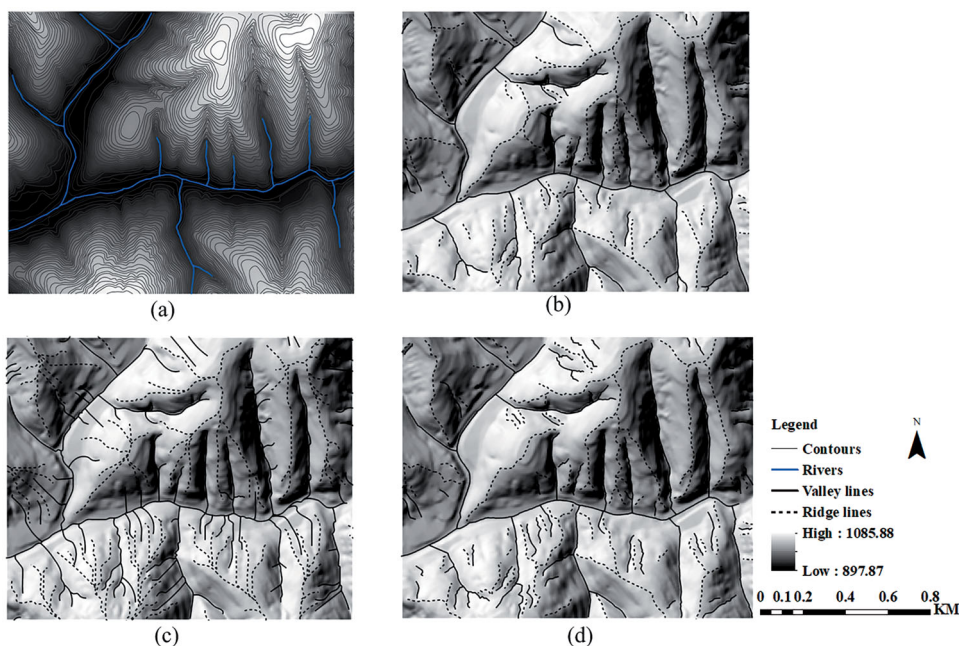


**Figure 14.** Original data from part of Shaanxi province of China and comparison results with different methods. (a) DEM with a resolution of 5 m, contours and rivers (scale 1:10,000). (b) The proposed method with  $k_1=0.3$ ,  $k_2=0.6$ ,  $k_3=0.05$  and  $k_4=0.05$ . (c) J–M method with tangential curvature threshold of 0.015 and accumulation threshold of 60. (d) Topographic feature lines generation by the Voronoi skeleton-based method.

difficult to group feature points and to extract topographic feature lines in follow-up study. If only a few are present, then some micro-geomorphologic features cannot be extracted completely. The larger the scale, the more prominent is the limitation. Second, to determine the more suitable weight coefficients corresponding to different landforms and map scale change, it may take some time for effectively analyzing the weight coefficients so as to obtain better results.

## 5. Conclusions and future work

In this study, we have introduced new multi-criterion methods to extract topographic feature line from contours on different topographic gradients. This work involves a number of steps. First, feature points are grouped based on the meaningful points selected by calculating the approximate mean curvature values for all vertices on the contours, and mountain tops and saddle points are found automatically to construct topographic feature lines as completely as possible. Second, the topological structure trees are established according to the relationships among the previously identified feature point groups. Then, the ‘mainstream’ and ‘hierarchical branches’ of the positive and negative topographic feature point groups are organized automatically. More importantly, multi-criterion methods are used to trace the topographic feature lines more accurately. Finally, all topographic feature lines (with the hierarchical structure) are extracted (Figure 10). Simultaneously, compared with RSG-based and Voronoi

skeleton-based methods, the proposed method can extract topographic feature lines with higher accuracy, better continuity, lower spatial logical conflicts between topographic feature lines and contours. Furthermore, the correct and hierarchical extraction of topographic feature lines has laid down a good foundation for multi-scale high-quality integrated generalization of contours and river systems.

For the future research, some related algorithms need to be improved. Besides that, on the basis of the source contour data and extraction of 3D topographic feature lines, contours and river systems can be generalized by using the 3D Douglas–Peucker algorithm (Fei and He 2009, He 2013) to overcome the occasionally present problems of geometrical position shifting and topological relationship variation after the automatic generalization of contours and river systems.

## Acknowledgements

The authors sincerely thank the editor and anonymous reviewers for their valuable comments and suggestions, which improved the quality of this article.

## Data and codes availability statement

The datasets and codes that support the findings of this study are available in *figshare.com* through the following link: <https://doi.org/10.6084/m9.figshare.15170058>.

## Disclosure statement

No potential conflict of interest was reported by the author(s).

## Funding

Funding was provided by the National Natural Science Foundation of China [Grant No. 41871378].

## Notes on contributors

**Lu Cheng** is a PhD student at School of Resource and Environmental Sciences of Wuhan University. Her research interest is 3D geographic information generalization.

**Qingsheng Guo** is a professor at School of Resource and Environmental Sciences and State Key Laboratory of Information Engineering in Surveying, Mapping and Remote Sensing of Wuhan University. His research interests are cartographic generalization, intelligent processing and visualization of geographic information.

**Lifan Fei** is a professor at School of Resource and Environmental Sciences of Wuhan University. His research interest is the generalization of geomorphology and river system.

**Zhiwei Wei** is a research assistant at Key Laboratory of Network Information System Technology (NIST), Aerospace Information Research Institute, Chinese Academy of Sciences. His research interests are map spatial cognition and knowledge mining, intelligent cartography, network geographic information service integration.

**Guifang He** is a lecturer at School of Geographic Information and Tourism of Chuzhou University. Her research is land informatization and cartography.

**Yang Liu** is a PhD student at School of Resource and Environmental Sciences of Wuhan University. His research interest is a progressive generalization of roads and buildings.

## ORCID

Qingsheng Guo  <http://orcid.org/0000-0001-5863-1946>

Zhiwei Wei  <http://orcid.org/0000-0002-3494-3686>

## References

- Ai, T., 2007. The drainage network extraction from contour lines for contour line generalization. *ISPRS Journal of Photogrammetry and Remote Sensing*, 62 (2), 93–103.
- Akima, H., 1970. A new method of interpolation and smooth curve fitting based on local procedures. *Journal of the ACM*, 17 (4), 589–602.
- Bai, X., Latecki, L., and Liu, W-y., 2007. Skeleton pruning by contour partitioning with discrete curve evolution. *IEEE Transactions on Pattern Analysis and Machine Intelligence*, 29 (3), 449–462.
- Band, L.E., 1986. Topographic partition of watersheds with digital elevation models. *Water Resources Research*, 22 (1), 15–24.
- Fei, L.F., 2002. *A method of cartographic displacement: on the relationship between streets and buildings*. Thesis (PhD). Hannover University.
- Fei, L.F. and He, J., 2009. A three-dimensional Douglas–Peucker algorithm and its application to automated generalization of DEMs. *International Journal of Geographical Information Science*, 23 (6), 703–718.
- Freeman, H. and Davis, L.S., 1977. A corner-finding algorithm for chain-coded curves. *IEEE Transaction on Computers*, C-26 (3), 297–303.
- Fukunaga, K. and Hostetler, L., 1975. The estimation of the gradient of a density function, with applications in pattern recognition. *IEEE Transactions on Information Theory*, 21 (1), 32–40.
- Guilbert, E., 2013. Multilevel representation of terrain features on a contour map. *Geoinformatica*, 17 (2), 301–324.
- He, J., 2013. Study on the method of indirect generalization for contour lines based on the 3D Douglas–Peucker algorithm. *Acta Geodaetica et Cartographica Sinica*, 42 (3), 467–473.
- Hooshyar, M.D., et al., 2016. Valley and channel networks extraction based on local topographic curvature and *k*-means clustering of contours. *Water Resources Research*, 52 (10), 8081–8102.
- Hu, P., et al., 2002. *Map algebra*. Wuhan: Publishing House of Wuhan University (in Chinese).
- Jasiewicz, J. and Metz, M., 2011. New GRASS GIS toolkit for Hortonian analysis of drainage networks. *Computers & Geosciences*, 37 (8), 1162–1173.
- Jin, H. and Gao, J., 2005. Research on the algorithm of extracting ridge and valley lines from contour data. *Geo-Spatial Information Science*, 8 (4), 282–286.
- Koenders, R., et al., 2014. Multi-scale curvatures for identifying channel locations from DEMs. *Computers & Geosciences*, 68, 11–21.
- Lashermes, B., Foufloula-Georgiou, E., and Dietrich, W.E., 2007. Channel network extraction from high resolution topography using wavelets. *Geophysical Research Letters*, 34 (23), L23S04.
- Luo, W. and Stepinski, T., 2008. Identification of geologic contrasts from landscape dissection pattern: an application to the Cascade Range, Oregon, USA. *Geomorphology*, 99 (1–4), 90–98.
- Mark, D.M., 1984. Automated detection of drainage network from digital elevation model. *Cartographica*, 21 (2–3), 168–178.
- Molloy, I. and Stepinski, T.F., 2007. Automatic mapping of valley networks on Mars. *Computers & Geosciences*, 33 (6), 728–738.
- Montgomery, D.R. and Dietrich, W.E., 1992. Channel initiation and the problem of landscape scale. *Science*, 255 (5046), 826–829.

- Montgomery, D.R. and Foufoula-Georgiou, E., 1993. Channel network source representation using digital elevation models. *Water Resources Research*, 29 (12), 3925–3934.
- O'Callaghan, J.F. and Mark, D.M., 1984. The extraction of drainage networks from digital elevation data. *Computer Vision Graphics, and Image Processing*, 28 (3), 323–344.
- Passalacqua, P., et al., 2010. A geometric framework for channel network extraction from lidar: nonlinear diffusion and geodesic paths. *Journal of Geophysical Research*, 115 (F1), 73–78.
- Peckham, S.D., 1995. *Self-similarity in the three-dimensional geometry and dynamics of large river basins*. Thesis (PhD). University of Colorado Montgomery.
- Pelletier, J.D., 2013. A robust, two-parameter method for the extraction of drainage networks from high-resolution digital elevation models (DEMs): evaluation using synthetic and real-world DEMs. *Water Resources Research*, 49 (1), 75–89.
- Petitjean, M. and Saporta, G., 1992. On the performance of peeling algorithm. *Applied Stochastic Models and Data Analysis*, 8 (2), 91–98.
- Qiao, C.F., et al., 2005. A method for generating contour tree based on Voronoi interior adjacency. *Geo-Spatial Information Science*, 8 (4), 287–290.
- Tang, G., Li, F., and Liu, X., 2010. *Digital elevation model tutorial*. Beijing: Science Press (in Chinese).
- Tarboton, D.G., Bras, R.L., and Rodriguez-Iturbe, I., 1991. On the extraction of channel networks from digital elevation data. *Hydrological Processes*, 5 (1), 81–100.
- Weibel, R., 1992. Model and experiments for adaptive computer-assisted terrain generalization. *Cartography and Geographic Information Systems*, 19 (3), 133–153.
- Xiong, H. and Li, X., 2015. A new method to extract topographic ridge lines and valley lines. *Geomatics and Information Science of Wuhan University*, 40 (4), 498–502.
- Xu, Q.R., et al., 1993. *The principles of computer cartography*. Wuhan: Press of the Wuhan Technical University of Surveying and Mapping (in Chinese).
- Zheng, X., et al., 2015. A robust channel network extraction method combining discrete curve evolution and the skeleton construction technique. *Advances in Water Resources*, 83, 17–27.